Vibrational and Thermodynamic Properties of H2 Adsorbed on MgO in the 300−20 K Interval

ARTICLE *in* THE JOURNAL OF PHYSICAL CHEMISTRY B · SEPTEMBER 2004

Impact Factor: 3.3 · DOI: 10.1021/jp0487410

6 AUTHORS, INCLUDING:

Serena Bertarione
TitaC srl
50 PUBLICATIONS **768** CITATIONS
SEE PROFILE

Domenica Scarano
Università degli Studi di Torino
144 PUBLICATIONS **3,916** CITATIONS
SEE PROFILE

Giuseppe Spoto
Università degli Studi di Torino
187 PUBLICATIONS **7,094** CITATIONS
SEE PROFILE

A. Zecchina
Università degli Studi di Torino
560 PUBLICATIONS **19,907** CITATIONS
SEE PROFILE

Vibrational and Thermodynamic Properties of H_2 Adsorbed on MgO in the 300−20 K Interval

Evgueni N. Gribov, Serena Bertarione,† Domenica Scarano,† Carlo Lamberti,† Giuseppe Spoto,*,† and Adriano Zecchina*,†

Dipartimento di Chimica IFM dell'Università di Torino, Via P. Giuria 7, I-10125 Torino, Italy

Received: March 22, 2004; In Final Form: July 20, 2004

The adsorption of H_2 on high surface area, sintered and smoke MgO samples fully characterized by HRTEM and AFM microscopies has been investigated in the 300−20 K temperature interval by FTIR spectroscopy On high surface area MgO, dissociative adsorption of H_2 has been observed with formation of reversible (absorbing at 3454 and 1325 cm^{-1}) and irreversible (absorbing at 3712 and 1125 cm^{-1}) OH and MgH species already reported in previous studies at 300 K. Cooling the MgO/H_2 system down to 20 K results in the irreversible formation at about 200 K of new OH (absorbing at 3576−3547 cm^{-1}) and MgH (absorbing at 1430−1418 cm^{-1}) surface groups never observed before. The spectra recorded at 20 K in H_2 atmosphere also show absorptions in the 4800−4000 cm^{-1} frequency interval undoubtedly due to molecularly adsorbed species. Decreasing the MgO surface area results in the disappearance of all of the spectroscopic manifestations due to the hydride and hydroxyl groups formed upon dissociative adsorption of hydrogen, whereas those due to H_2 adsorbed in molecular form are maintained (although with much reduced intensity). This behavior is the consequence of the reduction, revealed by HRTEM and AFM, of the concentration of surface defects (cationic and anionic sites located on edges, corners, steps, inverse edges and inverse corners). On the basis of the morphological characterization and of the IR spectroscopic studies, it is concluded that the sites responsible for the H_2 dissociative adsorption are mainly inverse steps "coupled" with edges and corners, whereas more usual "isolated" defects (edges, steps, and corners) adsorb hydrogen only in molecular form. The specific adsorption energy for the formation of molecular $Mg_{nC}^{2+}\cdots H_2$ adducts on Mg_{3C}^{2+} (corners; 7.5 kJ/mol), Mg_{4C}^{2+} (edges; 4.6 kJ/mol), and Mg_{5C}^{2+} (on (100) planes; 3.6 kJ/mol) coordinatively unsaturated sites has been also calculated from the temperature dependence of the intensity of the related IR bands (ν(HH) mode).

Introduction

The study of H_2 adsorption on oxides is of relevant importance within the framework of the vast theme of hydrogen activation on solid surfaces, finding application in catalysis[1] and hydrogen storage.[2]

As far as catalysis is concerned, hydrogenation, dehydrogenation, and hydrogen transfer reactions are known to occur at the surface of α-Cr_2O_3 and other oxides containing transition metal ions with a partially filled d shell.[1] Systems incorporating metal ions in d^{10} or d^0 electronic configuration (either metal oxides such as ZnO or MgO or oxidic materials such as exchanged zeolites) are generally less active but nevertheless important, at least for fundamental studies, because of their ability to dissociate the hydrogen molecule. The investigation of the surface properties of oxides toward the H−H bond activation is also of importance because of the analogies with the C−H bond activation, a topic occupying a central position in industrial processes. In this respect, it has been for instance shown that the sites responsible for H_2 dissociation on MgO are also active in the C−H cleavage.[3]

Coming to hydrogen storage, the possible use of high surface area oxidic systems has been proposed because of their adsorptive ability.[2,4,5] It is however a matter of fact that to make these materials really attractive for practical usage an increase is needed of the amount of hydrogen stored per unit weight via dissociative or molecular paths. To attain this goal, a better knowledge of the structure and of the forces involved in the physical (molecular) and chemical (molecular and/or dissociative) adsorption processes is in turn required. In the case of molecular adsorption, new information can be achieved by studying the perturbation induced on H_2 by the interaction with the surface. The modification of the infrared spectrum of adsorbed hydrogen (in terms of frequency and intensity of the absorption bands with respect to the free molecule) is particularly informative because it allows the determination of the strength of the interaction, as well as to gain information on the structure of the active surface sites and on the role of the involved chemical and electrostatic forces.[6,7] Vibrational spectroscopy has also proved its utility when dissociative adsorption is occurring, because the formed hydride and hydroxylic species are characterized by well-defined IR peaks.[8,9] When molecular and dissociated forms are both present on the surface, the interpretation of the IR spectra can become quite complex and the assignment problematic. This is particularly true when heterogeneous surfaces are involved.[10,11] In this contest, the study of the IR spectroscopy of hydrogen adsorbed on oxides characterized by well-defined morphology (like MgO and ZnO) and hence representing reference systems can be of fundamental importance.[1,8,9,12−16]

* To whom correspondence should be addressed. E-mail: giuseppe.spoto@unito.it (G.S.); adriano.zecchina@unito.it (A.Z.).

† Consorzio Interuniversitario Nazionale per la Scienza e la Tecnologia dei Materiali (INSTM) (http://www.cineca.it/hosted/incm/instm/) and Nanostructured Surfaces and Interfaces−Centre of Excellence (NIS) (http://www.nis.unito.it/).

10.1021/jp0487410 CCC: $27.50
Published on Web 09/18/2004

SCHEME 1

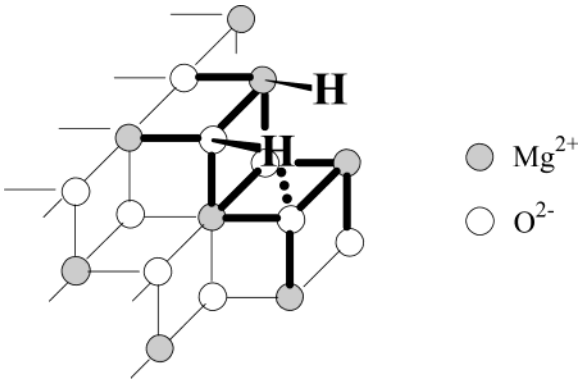

Focusing on the H_2/MgO interaction, let us recall that hydrogen adsorption on this solid can in principle be either molecular or dissociative. Dissociative adsorption of hydrogen on high surface area MgO has been already reported and two different paths proposed: *homolytic* and *heterolytic*.[1] Homolytic splitting is supposed to operate under UV-irradiation only[15,17,18] and will not be further discussed here. Heterolytic splitting takes place in the dark and at 300 K on coordinatively unsaturated (*cus*) $Mg^{2+}O^{2-}$ surface pairs following the schematic mechanism illustrated below:

$$-\,Mg^{2+}_{cus}O^{2-}_{cus}\,- \;+\; H_2 \;\rightarrow\; -\,\overset{H^-}{Mg^{2+}_{cus}}\,\overset{H^+}{O^{2-}_{cus}}\,-$$

By this process two different families of hydrides and hydroxyls groups are formed differing for their vibrational properties and their behavior upon changes of the H_2 equilibrium pressure.

The first family is characterized by two intense and narrow IR peaks at 1325 (ν(MgH) stretching mode) and 3462 cm^{-1} (ν(OH) mode). These dissociatively adsorbed species are reversible at room temperature upon reducing the H_2 pressure: this suggests that the two fragments are either in adjacent position or, if adsorbed at distant positions, capable to easily migrate on the surface to recombine and give back molecular hydrogen.[8,9,19] Concerning the nature of the surface centers responsible for the splitting, Knözinger et al.[9] first hypothesized that the adsorbing ions are in 3-fold coordination as represented in Scheme 1. The H^+ fragment is actually in doubly bridged position so explaining the rather low frequency (3462 cm^{-1}) of the ν(OH) mode.[8,9] The driving force for the dissociation is considered to be associated with the high nucleophilicity of the low coordinated oxygen ion and the strong Lewis acidic character of the adjacent Mg^{2+} cation. The hypothesis that low coordinated sites are involved is supported by the observation that hydrogen dosage at room temperature leads to the partial erosion of the UV transition assigned to 3-fold coordinated O^{2-} sites.[3,19]

Following Paganini et al.,[20] a more general representation of the structure involved in the heterolytic splitting is the following:

$$\square(Mg^{2+})_{LC}(O^{2-})_{LC}$$

where $\square$ is a surface oxygen vacancy and LC stands for low coordination.

The whole problem of the hydrogen adsorption on MgO has been recently reconsidered by Ricci et al.[21] suggesting as a working hypothesis that inverse corner sites present at monatomic steps intersections play a role in both reversible and irreversible (vide infra) dissociative hydrogen adsorption, as shown in Scheme 2.

SCHEME 2

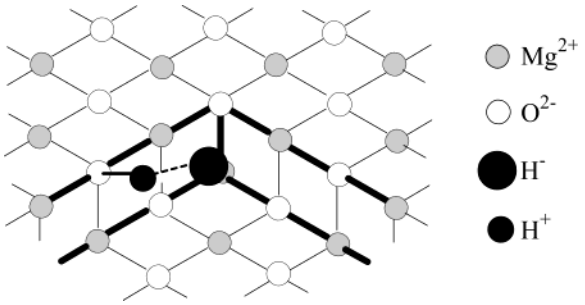

Following their model, the H^- fragment formed by heterolytic splitting is located at anionic-type vacancies present at inverse corner sites (multibridged hydride species), whereas the H^+ is adsorbed on 4-fold coordinated O^{2-} sites generating a protruding OH group.[21]

Going to the second family of hydride and hydroxyls groups formed upon hydrogen adsorption at room temperature, it is responsible for two absorptions at 1125 (ν(MgH), broad) and 3712 cm^{-1} (ν(OH), sharp). The intensity of these bands is critically dependent upon the surface area and the outgassing temperature, as the responsible species can be desorbed from the surface only at temperature comprised in the 300−400 K interval.[9] Following Ricci et al.[21] also the 3712−1125 cm^{-1} doublet is the result of a heterolytic splitting process occurring at inverse corner sites. This conclusion is in our opinion very reasonable, and we shall try to confirm it on the basis of new data obtained upon interaction of H_2 with MgO in the 300−20 K temperature interval.

As far as the possibility of molecular adsorption of H_2 on the cationic and/or anionic surface centers of MgO, it is worth underlining that species of this kind have never been observed so far, even though it is known that H_2 can interact with a variety of charged centers like (i) bare cations [In this respect, we recall that the stability of dihydrogen complexes of Li^+, Na^+, HMg^+, H_2Al^+, etc. has been ascertained by theoretical calculations [22] but also finds support in some experimental results.[23]]; (ii) coordinatively unsaturated sites at the surface of ionic solids [In this field special mention must be made about the results obtained on the H_2/NaCl system in the 20−12 K interval.[24−28]]; (iii) cationic sites or acid−base couples in alkali-exchanged[6,29−35] and protonic[36] zeolites or zeotypes;[7] (iv) metalorganic frameworks.[5]

In all of the cases, the interaction of H_2 with the adsorbing centers is electrostatic in nature and results in the perturbation of the ν(HH) mode which becomes infrared active and shifted to lower frequency with respect to the free molecule. As it will be shown here, the lack of experimental evidence of H_2 molecular adsorption on MgO is due to the temperature (300 K) of the past experiments, which was too high for such weak interaction.

In the present work, the adsorption of hydrogen on MgO has been investigated by FTIR spectroscopy in the whole temperature range from 300 to 20 K with the aim of getting a better insight into the nature and the formation mechanisms of surface O−H and Mg−H groups generated by H_2 splitting as well as into the structure of the involved surface centers. A second objective was to explore the possibility of formation, in favorable experimental conditions (adsorption temperature as low as 20 K), of molecularly adsorbed species, which could possibly help to better understand the complex surface properties of this oxide.

These goals were attained by a careful study of the FTIR spectra of H_2 adsorbed on MgO samples characterized by different specific surface area and fully characterized by microscopic techniques (HRTEM and AFM). Recording of the IR bands intensity at variable temperature also allowed us to evaluate some thermodynamic properties of the molecularly adsorbed surface species which cannot be obtained by calorimetric techniques because of the very unfavorable conditions at which molecular adsorption take place (ca. 20 K). Moreover, this spectroscopic method allowed us to separately estimate the adsorption energy at specific surface sites differing for the coordinative unsaturation degree.[35,37]

Experimental Section

Hydrogen adsorption was studied on three different MgO polycrystalline samples characterized by decreasing surface areas (~230, ~40, and ~10 m^2/g). High surface area (~230 m^2/g, hereafter *hsa*) MgO was obtained by careful decomposition of $Mg(OH)_2$ at 523 K in vacuo. Low surface area (~10 m^2/g, hereafter named as *smoke*) MgO was produced by direct combustion of Mg ribbon in air. Samples with intermediate surface area (ca. ~40 m^2/g) were prepared upon sintering *hsa* MgO at 1073 K according to the procedure described elsewhere[37] and will be hereafter named as *sintered* MgO. Before the H_2 adsorption experiments, all of the samples were pressed in into pellets suitable for transmission infrared measurements and outgassed in vacuo (final pressure $< 10^{-5}$ mbar) at 1073 K for 2 h. After this treatment no traces of chemisorbed water (or other adsorbed impurities) were detectable in MgO infrared spectrum.[38,39]

The infrared spectroscopic measurements were performed using a properly designed cryogenic cell allowing (i) the in situ high-temperature activation (up to 1073 K) of the sample under high vacuum condition (or in desired atmosphere); (ii) to perform FTIR adsorption experiments at fixed temperature, as low as ca. 20 K (estimated at the sample level), and variable H_2 pressure; (iii) to record the IR spectra of the species adsorbed in the whole from 300 to 20 K temperature interval while simultaneously measuring the gas-phase equilibrium pressure, a procedure which allows us to obtain the site-specific adsorption enthalpy.

A detailed description of the cryogenic cell (consisting of a properly modified closed circuit liquid helium Oxford CCC 1204 cryostat) is given elsewhere.[37] The spectra were acquired in the 5000−750 cm^{-1} frequency interval at a resolution of 1 cm^{-1} by averaging 128 interferograms on a Bruker Equinox-55 FTIR spectrometer whose sample compartment was modified ad hoc to accommodate the cryogenic IR cell. All of the spectra reported in the following are background subtracted using the spectrum of pure MgO as reference.

AFM (atomic force microscopy) images of *smoke* MgO were obtained on a Park Scientific Instrument Auto Probe LS, equipped either with high aspect ratio silicon conical tips, operating in the repulsive force (contact) mode (by the so-called constant force mode (16 N/m), with scanning frequencies of 0.5 and 1 Hz), or with silicon nitride pyramidal tips, operating in noncontact and tapping modes (force constant = 0.05 N/m). Atomic scale images were obtained in contact mode regime, using pyramidal tips; the typical applied force between the tip and the sample surface was of the order of 1.399 nN. All of the AFM images were recorded in air at room temperature; the MgO sample was in the form of a film obtained by directly collecting on a cold support the magnesium oxide dust produced by combustion of metal Mg.

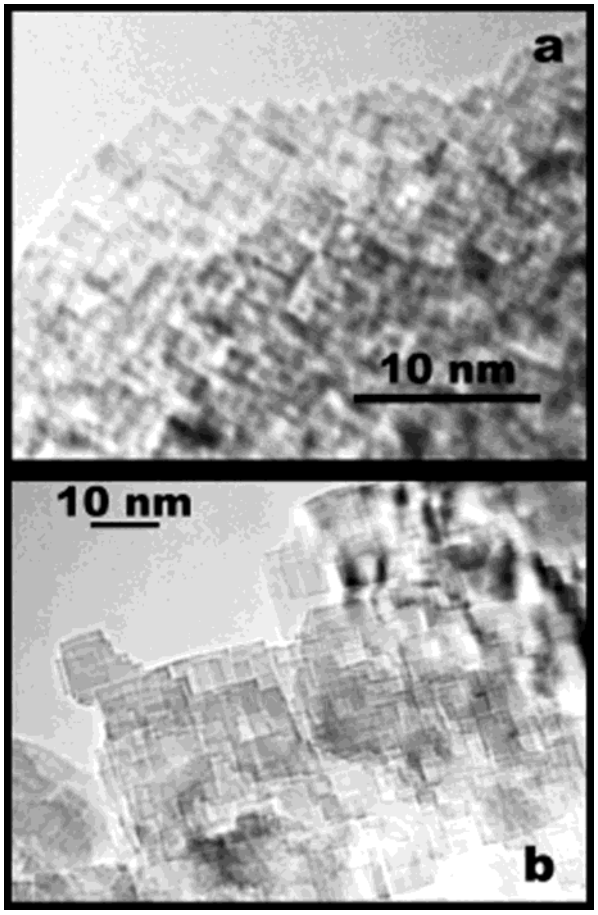

Figure 1. HRTEM images of high surface area (a) and sintered (b) MgO samples (notice the different magnification in the two plates).

Transmission electron micrographs were obtained with a JEOL JEM 2000EX HRTEM microscope, equipped with a top-entry stage and operating at 200 kV. The MgO samples were in powdered form, simply dispersed on holey-carbon sample grids without any further manipulation or treatment.

Results

Morphology of the MgO Samples. It is widely accepted that on *hsa* (high surface area) MgO the concentration of surface defects (edges, steps, and corners) reaches a maximum: this explains the complexity of the IR spectra of adsorbed CO[1,37] and of dissociatively adsorbed hydrogen published so far and the difficulties encountered in the vibrational assignment.[1] This consideration has prompted us to study the dependence of the spectroscopic manifestations of adsorbed hydrogen upon the morphology of the MgO particles. It is in fact expected that a gradual and controlled decrement of the defects concentration should be associated with the parallel decrement of the number of the surface species formed by adsorption and hence by a simplification of the spectra. To achieve this goal, we have progressively sintered under controlled temperature conditions the *hsa* oxide initially prepared by decomposition under vacuum of $Mg(OH)_2$, so obtaining MgO samples characterized by surface area gradually changing from ~230 to ~40 m^2/g and hence characterized by progressively better defined morphology. The morphology of two of these samples, as studied by high-resolution transmission electron microscopy (HRTEM), is illustrated in Figure 1.

From Figure 1 it is inferred that the MgO microcrystals are constituted by small interpenetrated cubes of dimension increas-

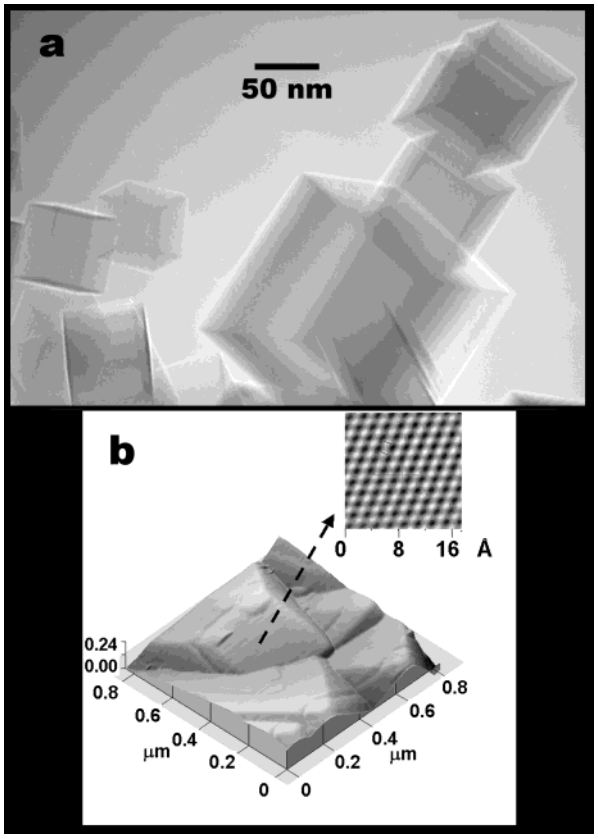

Figure 2. HRTEM (a) and large scale topography AFM (b) images of a freshly prepared MgO *smoke* sample. In the inset of part (b) an atomic scale AFM image of a portion of an extended (100) surface is reported (deviation from perfect square symmetry due to piezo creep). The image in (b) was obtained on the film obtained by collecting, directly on the platelet used for the AFM experiment, the cloud of microparticles which are formed by burning Mg metal in air; image (a) on the same sample but in powdered form.

ing with sintering. It is noticeable that together with defective structures such as corners, edges, and flat surface portions (constituted by (100) planes), the microcrystals also contain in abundance terraces, steps, inverse steps of variable height, and inverse corners (following the definition of Ricci et al,[21] vide also Figure 3). In particular, inverse steps and inverse corners represent the real peculiarity of these high surface area systems.

As it is possible to see in part (a) of Figure 2, these sites cannot be found on samples constituted by individuals cubes of variable dimension like those obtained by combustion of Mg metal in air (*smoke* MgO). It is in fact evident from Figure 2a that freshly prepared MgO *smoke* is formed by separated cubic microparticles, delimited by exposed (100) planes, of great morphological perfection with no or very few signs of interpenetration, i.e. with vanishingly small concentration of steps, inverse steps and inverse corners.[37] The perfection of the (100) faces of the individual microcrystals is further demonstrated by the atomic force microscopy (AFM) reported in part (b) of Figure 2, where a large scale topography of a portion of the (100) extended surface is imaged (deviation from perfect square symmetry being due to piezo creep): this image resolved at atomic scale (inset) of the particles surface allows us to appreciate the absence even of point defects.

Of course, we have to consider the possibility that during the activation at high temperature in a vacuum (dehydroxylation) some of the original MgO *smoke* cubic particles (in particular the smallest ones) can establish chemical contacts with the largest ones (interpenetration). In this respect, analysis of the

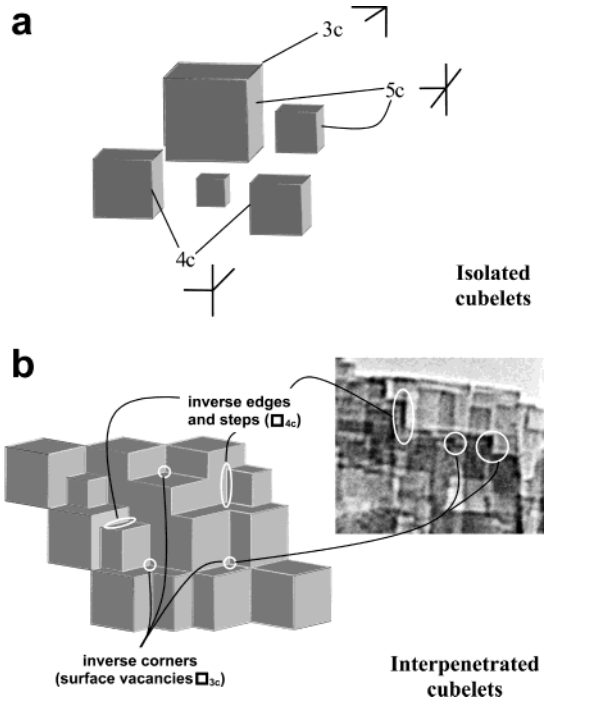

Figure 3. Schematic representation of morphological changes on passing from *smoke* (a) to *hsa* MgO (b). On the isolated cubic microcrystals of MgO *smoke* (a) surface ions are located on corners (3c: triply coordinated), edges (4c) and (100) faces and terraces (5c). *hsa* MgO (b) consists of interpenetrated small cubes and new defective sites appear (inverse corners and inverse steps). Defects of this type are easily individuated in the HRTEM image (actually a detail of the micrograph of Figure 1b) reproduced in (b) on the right.

HRTEM images of the *smoke* sample after activation indicates that the vast majority of cubes still maintain their individual character (micrograph not reported for brevity). We so conclude that interpenetration is negligible not only on freshly prepared samples but also on those activated at high temperature. A schematic representation of the structural situations differentiating the *hsa* samples obtained by $Mg(OH)_2$ decomposition, constituted by interpenetrated small cubes and by presence of inverse corners and steps, and *smoke* is given in Figure 3.

As evidenced in Figure 3a, the surface sites present on MgO *smoke* are (i) tri-coordinated Mg_{3c}^{2+} and O_{3c}^{2-} ions (where +2 and −2 have to be intended as formal charges) located at the corners of the cubes, whose spatial separation is of the order of some 10 nm (as estimated form Figure 2a); (ii) tetracoordinated Mg_{4c}^{2+} and O_{4c}^{2-} ions located on steps; and (iii) pentacoordinated Mg_{5c}^{2+} and O_{5c}^{2-} ions located on (100) faces and terraces. On *hsa* MgO (ex $Mg(OH)_2$), the situation is distinctly different because, beside the previously mentioned sites which are now present with increased concentration, new surface defects must be considered as well named "inverse corners" and "inverse edges". These sites can be regarded as pseudo-surface vacancies □ able to accumulate positive (H^+) and negative (H^-) fragments formed upon heterolytic splitting of hydrogen (the term pseudo-vacancies is used to mean that we are dealing with surface morphological defects not altering the electrical neutrality of the solid). The adsorbed H^+ fragments should have the spectroscopic features typical of hydroxyl groups, because the vibrations involve the stretching of OH bonds; for instance:

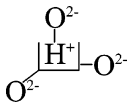

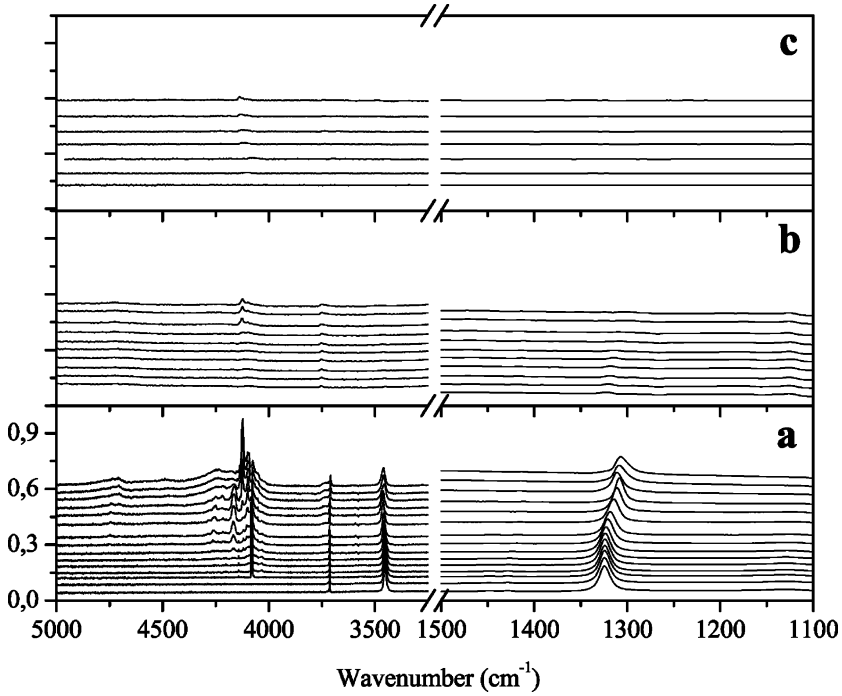

Figure 4. Pressure dependence of the IR spectra of H_2 adsorbed at 20 K on (a) *hsa*, (b) *sintered*, and (c) *smoke* MgO samples previously outgassed in vacuo at 1073 K. The upper curve of each series is the spectrum at maximum coverage (H_2 equilibrium pressure 10 mbar), the bottom curve that recorded after prolonged outgassing at 20 K (residual equilibrium pressure $< 10^{-3}$ mbar). All spectra have been vertically shifted for sake of clarity. The ordinate scale is the same in the three parts.

whereas the adsorbed H^- fragments should have the spectroscopic properties of bridged (and ionic vide infra) hydride species; for instance:

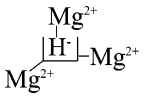

Although the fragments located at inverse corners are triply bridged (*vide* schemes above) and presumably under ionic form, those sited at inverse steps are doubly bridged and characterized by more covalent bonds.

Vibrational Spectroscopy of H_2 Adsorbed in the 300−20 K Interval and the Influence of the Sample Morphology. The spectra of H_2 adsorbed at 20 K on MgO samples (previously outgassed in vacuo at 1073 K) of different surface area (*hsa*, *sintered*, and *smoke*) are compared in Figure 4; in all cases, the spectral series were obtained upon dosage on the MgO pellet pre-cooled at 20 K of a quantity of H_2 corresponding to an equilibrium pressure of 10 mbar and by successive reduction of the pressure in step at the same temperature. For each series in Figure 4, the upper spectrum corresponds to maximum coverage and was always obtained after allowing the MgO/H_2 systems to reach equilibrium conditions, i.e., after waiting for about 1 h at constant H_2 pressure and temperature. For the sake of clarity, the evolution of the spectra in this time interval will be considered and discussed later. The less intense spectra in Figure 4 corresponds to a residual equilibrium pressure lower than 10^{-3} mbar; the remaining curves to intermediate pressure conditions.

An exploded view of the sequence obtained on the *hsa* MgO/H_2 system is illustrated in Figure 5, whereas Figure 6 shows a similar series obtained on the same kind of sample (*hsa* MgO) but by a different experimental procedure, consisting of (i) dosage of hydrogen at 300 K, (ii) cooling of the MgO/H_2 system down to 20 K, and (iii) stepwise reduction of the H_2 equilibrium pressure at the same temperature (actually only the spectra obtained in this last part of the experiment are illustrated in Figure 6).

On the basis of Figures 4-6, the following can be commented:

(a) The overall intensity of the IR manifestations of hydrogen adsorbed at 20 K decreases strongly on passing from the *hsa* sample to *smoke* (Figure 4) as a consequence of the specific surface area decrement (from ∼230 to ∼10 m^2/g). The decrease in intensity is definitely more pronounced for the bands comprised in the 3800−3400 and 1500−1100 cm^{-1} ranges. This results, together with the morphological changes observed by HRTEM (Figures 1 and 2), leads to the conclusion that the sites responsible for the absorptions in these regions, being preferentially annealed by sintering, involve highly coordinatively unsaturated surface ions (like those present on corners, steps, etc.).

(b) The spectra in the 3800−1100 cm^{-1} range depend on whether hydrogen is initially dosed on MgO at 20 K (Figure 5) or at 300 K and then cooled to 20 K (Figure 6). In both the cases, however, several bands are observed which are due to the stretching modes of a variety of hydroxyl (absorptions in the 3800−3400 cm^{-1} interval) and hydride species (absorptions in the 1500−1100 cm^{-1} interval).

(c) The ν(OH) band at 3454 and that due to the ν(MgH) mode at 1325 cm^{-1} (present in Figure 5 as well as in Figure 6) are the same already discussed in the literature for hydrogen adsorption at room temperature through the heterolytic path.[8,9] Their formation even at temperature as low as 20 K indicates that the involved sites are very active toward H_2 dissociation. As it will be shown in the following formation of these species at 20 K occurs through a molecularly adsorbed precursor. For equilibrium pressures increasing from ca. 0.5 to 10 mbar (i.e., in the pressure range where the molecularly adsorbed species absorbing at frequencies >4000 cm^{-1} are formed, vide infra),

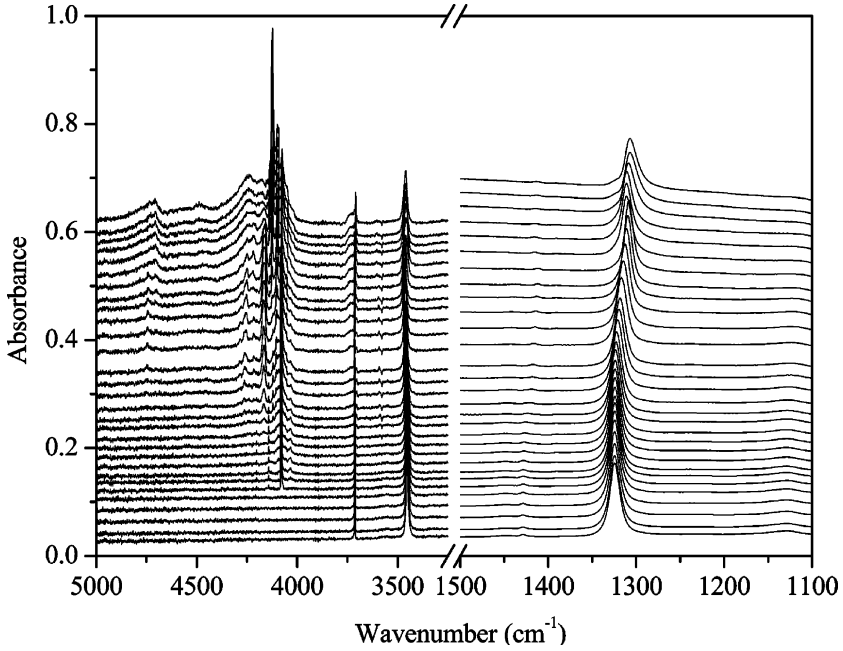

Figure 5. Dependence on the equilibrium gas pressure of the IR spectra of H_2 adsorbed at 20 K on *hsa* MgO. Uppermost curve: 10 mbar H_2 at 20 K; other curves: effect of gradual lowering the hydrogen pressure at the same temperature (final pressure $< 10^{-3}$ mbar).

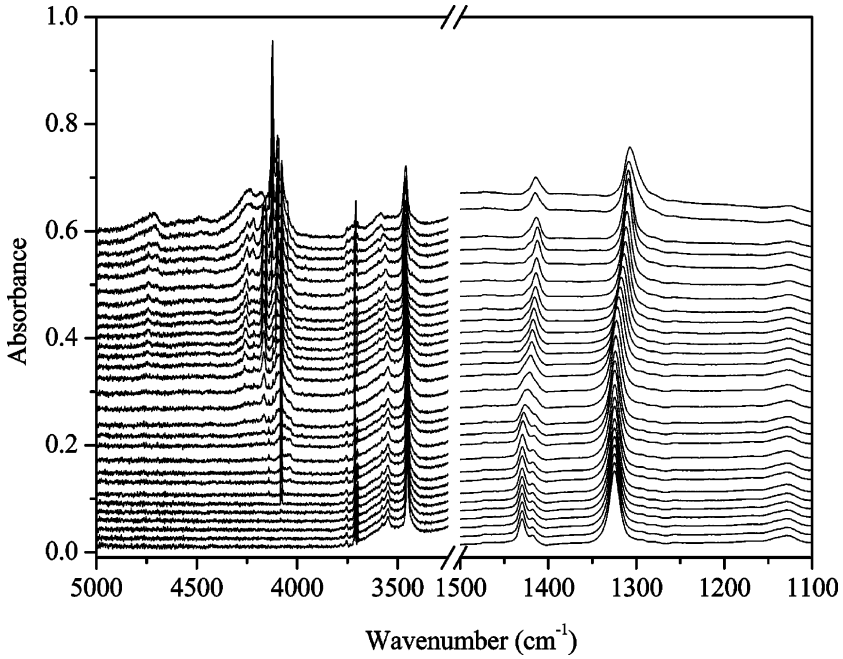

Figure 6. Pressure dependence at 20 K of the IR spectra of H_2 first adsorbed on *hsa* MgO at 300 K and then cooled to 20 K. Upper curve: spectrum at 20 K at maximum H_2 coverage (equilibrium pressure 10 mbar); other curves: effect of gradual lowering the hydrogen pressure at the same temperature (final pressure $< 10^{-3}$ mbar).

these peaks become broader and move simultaneously upward (from 3454 to 3460 cm^{-1}) and downward (from 1325 to 1306 cm^{-1}), the two shifts being linearly correlated. Both species are irreversible at 20 K, while outgassing at room temperature leads to their total disappearance.[8,9]

(d) The peaks at 3712 and at 1125 cm^{-1} (present in both Figures 5 and 6) correspond to a second family of OH and MgH groups. Also these species, which are irreversibly adsorbed at 20 K as well as at 300 K, are already formed at 20 K and are hence generated on a very active sites (other than previous). Unlike for the 3454−1325 cm^{-1} doublet, it was not possible to identify any molecular precursors (even at 20 K); another difference is the little tendency of the 3712−1125 cm^{-1} doublet to shift upon increasing the hydrogen pressure.

(e) The spectra of Figure 6 show that beside the hydroxyl peaks at 3712 and 3454 cm^{-1} and the hydride peaks at 1325 and 1125 cm^{-1}, new (never described before) OH/MgH pairs at 3576−3547 (doublet) and at 1430−1418 cm^{-1} (doublet) are present when the sample is contacted with H_2 at 300 K and then cooled in H_2 atmosphere down to 20 K. It is worth underlining that these peaks are not formed at room temperature but only appear at about 200−180 K while progressively cooling the H_2/MgO system: this explain why they were not observed in previous studies all performed at 300 K. The formation of these bands is however inhibited when H_2 is dosed at 20 K (Figure 5). We can therefore conclude that the responsible species are formed through an activated process on sites starting to be populated by H_2 only below room temperature (at 200−

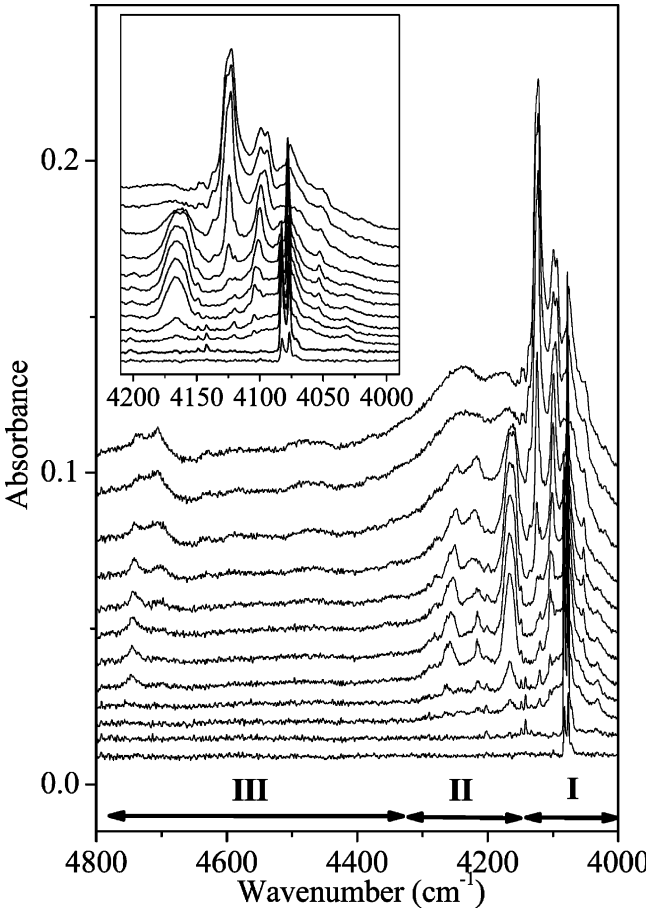

Figure 7. Pressure dependence (at 20 K) of the spectrum of hydrogen molecular species adsorbed on *hsa* MgO. The H_2 equilibrium pressure is decreasing from the upper curve (10 mbar) to the lower ($<10^{-3}$ mbar). (**I**) ν(HH) region; (**II**) region of the combinations ν(HH) + external (translational) modes; (**III**) region of the roto-vibrational modes. An enlargement of the 4200−4000 cm^{-1} interval is given in the inset.

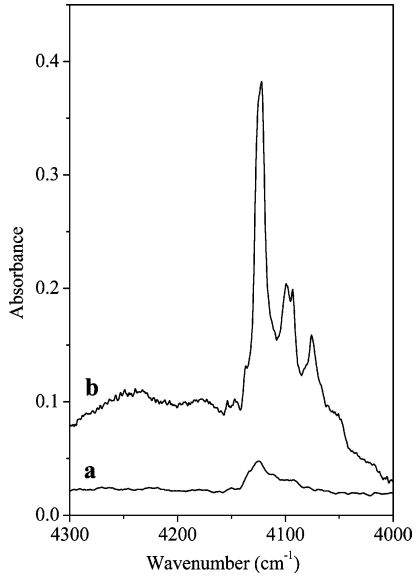

Figure 8. IR spectra in the ν(HH) region of H_2 adsorbed at 20 K (equilibrium pressure 10 mbar) on (a) *smoke* and (b) *hsa* MgO.

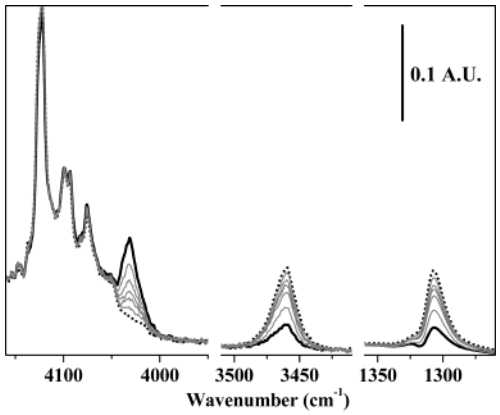

Figure 9. Dependence on the contact time of the spectrum of H_2 adsorbed at 20 K on *hsa* MgO. For clarity, only the ν(HH) (4160−3950 cm^{-1}), ν(OH) (3520−3380 cm^{-1}) and the ν(MgH) (1360−1260 cm^{-1}) regions are shown. Heavy full line: immediately after the dosage of 10 mbar of H_2 on the sample pre-cooled at 20 K. Heavy dotted line: after 1 h of contact at 20 K. Light lines: intermediate contact times.

180 K). These peaks are irreversible at 20 K and shift upward and downward respectively upon increasing the H_2 pressure. Their behavior is similar to that of the species described in (a).

(f) Upon increasing the H_2 coverage, a complex and intense spectrum develops on *hsa* MgO in the 4800−4000 cm^{-1} interval, constituted by numerous components at 4081−4075 (doublet), 4106−4100 (doublet), 4127−4122 (doublet), 4167, 4215, 4257, 4480 (very broad), 4705, and 4747 cm^{-1}, better appreciated in the exploded view in Figure 7. Comparison with the results obtained on the $NaCl/H_2$ system[24,25] definitely indicates that these manifestations are associated with hydrogen adsorbed in molecular form on (100) faces and terraces, higher index faces, edges, steps, corners, and other defects. The intensity of the various components decreases in a different way upon sintering, as shown in Figure 8, those at lower frequency being preferentially affected.

It is useful to recall at this point that the experiments illustrated in Figures 4−8 and discussed in the previous part show the effect of the H_2 pressure on the spectra of the molecularly and dissociatively adsorbed species after full equilibration of the H_2/MgO system at 20 K. It is however noticeable that, as already anticipated above, when hydrogen is dosed on *hsa* MgO pre-cooled at 20 K a dependence of the spectrum on contact time is observed before equilibration is reached. This effect is shown in Figure 9 where a spectral sequence is reported obtained by the following procedure: (i) the *hsa* MgO sample, previously treated in a vacuum at 1073 K, was cooled in He atmosphere (in order to favor thermal exchange) down to 20 K; (ii) He was then outgassed and hydrogen dosed (up to an equilibrium pressure of 10 mbar) on the sample maintained at 20 K; (iii) spectra were finally collected, at 20 K and constant pressure, at fixed time intervals (10 min) until no further changes were observable (equilibration conditions reached in about 60−70 min).

In these conditions, a new intense band, undoubtedly associated with a new molecularly adsorbed hydrogen species, is observed immediately after H_2 dosage at 4031 cm^{-1}. The intensity of this manifestation gradually decreases with time, demonstrating the transient nature of the responsible dihydrogen surface adducts. The disappearance of the 4031 cm^{-1} band is clearly accompanied by the parallel growth of the couple of absorptions at 3460 and 1306 cm^{-1} already assigned (vide supra) to OH and MgH species formed through heterolytic dissociation. In conclusion, the results of Figure 9 clearly demonstrate that the heterolytic splitting of the H_2 molecule is preceded by the formation of a molecular surface species only observable in very low-temperature conditions.

Discussion

Basic Spectroscopic Properties of Surface Hydrides, Hydroxyl Groups, and Dihydrogen Molecular Adducts. From the experiments described in the previous parts it can be concluded that by interaction of hydrogen with the surface of *hsa* MgO up to three families of hydride species and three families of hydroxyl groups can be formed. The frequencies of the hydroxyl groups are comprised in 3800−3400 cm^{-1} interval, whereas those of the hydrides span in the 1500−1100 cm^{-1} range. The adsorptive capability of the surface is not exhausted by the dissociative process: the surface is in fact still able to adsorb H_2 in molecular form. The molecularly adsorbed species give rises to a complex spectrum in the 5000−4000 cm^{-1} region.

To fully understand the structural implications of these spectroscopic features and to try their assignment to specific O^{2-}/Mg^{2+} defective surface structures compatible with the electron microscopy results, it is useful to shortly summarize and discuss the literature data concerning the IR properties of surface hydroxyl and hydride groups on a variety of solids (including MgO), as well as of H_2 molecular adducts.

Let us first consider the hydrides frequency. It is known that the ν(MH) mode (were M stands for metal) is very sensitive to the coordination (number of bridging ions) of the hydrogen atom and to the ionicity of the metal−hydrogen bond, these two factors often acting simultaneously and being correlated. The current opinion is that bridged hydrides are absorbing at frequencies lower than those located in terminal position.[40] As far as the ionic character of the hydride bond is concerned, the fact that it also plays an important role in determining the force constant of the vibration, and finally the frequency, is demonstrated by the succession $\nu(B^{III}H)$ (2650 cm^{-1}) > ν(GaH) > ν(ZnH) > ν(CuH) > ν(MgH) > ν(LiH) > ν(NaH) > ν(KH) > ν(RuH) > ν(CsH) (866 cm^{-1}). Indeed, the large variation (about 1800 cm^{-1} over the whole series) of the ν(MH) frequency can be understood only if the polar character of the bond and the shallower curvature of the potential associated with the M−H coordinate are strongly influencing the stretching frequency.[40] To understand the relative role of ionicity and bridging of the hydrogen atom in determining the $\bar{\nu}$ (MgH), let us observe that in the isolated MgH_2 molecule (where the hydrogen atoms are in terminal position) the Mg−H stretching modes are in the 1640−1610 cm^{-1} interval,[41,42] whereas in solid MgH_2 (where the H^- is bridged in planar configuration to three Mg^{2+} ions via highly polar bonds) the ν(MgH) is shifted to about 1160 cm^{-1}.[43] On this basis, it can be assumed that the shift induced on the Mg−H stretching frequency on passing from terminal to triply bridging situation is ca. −500 cm^{-1} and that this figure can be used to evaluate the coordination state of hydride species formed on MgO.

In principle, it is expected that also the ν(OH) frequency of the hydroxyl groups formed by interaction of the H^+ fragment with the O^{2-} ions could be diagnostic of the coordinative situation of the adsorbing oxygen sites. However, the problem of the relation between the ν(OH) frequency and the coordination state is controversial. For instance, Coluccia et al.[38] think that on the MgO surface the frequencies of the OH groups not involved in hydrogen bonding (either in terminal position or bridged to three Mg ions) are comprised in the quite narrow 3737−3690 cm^{-1} interval, the triply bridged OH species falling at lowest frequencies (possibly ca. 50 cm^{-1} downward shifted with respect to terminal groups). However, Knözinger et al.[39] consider also a peak at 3620 cm^{-1} as prototype of multiply bridged species and suggest that a shift of about −130 cm^{-1} with respect to isolated (terminal) OH groups is likely a more reasonable figure for multiple bridging. Shido et al.[44] think that the shift associated with multiple bridging of the OH groups must be extended up to −240 cm^{-1}. It must be finally noticed that, on the basis of data obtained on model compounds, some authors even conclude that the ν(OH) frequency increases with the number of coordinating cations,[45,46] so increasing the uncertainty about the relation between the shift of the OH mode and the number of bridging oxygens.

In our opinion, the most important factor determining the frequency of H^+ fragment adsorbed at negative sites is represented, as in the case of the H^-, by the number of O^{2-} anions interacting with it and by the bond ionicity. Moreover, like commented before for hydride species, we can further reasonably assume that the ionic character of the O−H bond and the bridging situation of the H^+ fragment are not separate factors. In particular, we can expect that the most covalent OH bonds (corresponding to protruding hydroxyls where the hydrogen atom is bonded to a single oxygen ion) should show the highest frequency. This hypothesis is fully substantiated by the observation that the protruding OH groups located at corner positions (which are the most resistant to outgassing at 1073 K) absorb at 3712 cm^{-1}.[38,39] On the contrary, when the H^+ fragment formed in the heterolytic dissociation process finds location at a cationic pseudo-vacancy (and hence interacts with two or three oxygen ions depending upon the structure of the vacancy), it is multiply bridged and the resulting O_nH (n = 2, 3) groups contain bonds characterized by increased ionicity. Both the factors (coordination number and ionicity) shift the frequency of the O−H vibration to lower values.

Moving to molecularly adsorbed species, it is useful to recall that the main features of the interaction of H_2 with bare cations, as emerging from theoretical[22] and experimental studies,[23] are the following: (i) the $M^+\cdots H_2$ complexes invariably have C_{2v} symmetry; (ii) the H−H stretching vibration is greatly influenced by the charge of the cationic center (the higher the charge, the lower being the ν(HH) frequency with respect to free H_2); (iii) reduction of the cationic charge through coordination of the cation with anions causes the weakening of the interaction (as, for instance, demonstrated by the higher ν(HH) frequency in the $F_3Al\cdots H_2$ complex with respect to the $Al^{III}\cdots H_2$).[48] Also the energetic of the dihydrogen complexes is strongly influenced by coordination. This is well demonstrated by comparing the calculated interaction energies (MP2 level of theory) of the $Mg^{2+}\cdots H_2$ (90 kJ/mol) and $F_2Mg\cdots H_2$ (10 kJ/mol) adducts.[47,48] As far as the Mg/H2 interaction is specifically concerned, let us finally recall that the formation of the $H_2Mg\cdots H_2$ dihydrogen complex in cryogenic matrixes has been also reported.[42]

Surface cations are also thought to be the most probable adsorption sites also in the case of molecular hydrogen complexes formed at the surface of ionic solids such as NaCl (although adsorption on anionic defective sites has been sometime proposed).[23,26,27] The main spectroscopic features for such kind of interaction can be summarized as follows: (i) the IR inactive stretching modes of *para*- (nuclear momentum I = 0; 25% in the gas phase, $\bar{\nu}$ (HH) = 4161 cm^{-1}) and *orto*-H_2 (I = 1; 75% in the gas phase, $\bar{\nu}$ (HH) = 4155 cm^{-1}) become IR active upon adsorption; (ii) the absorptions of both H_2 species adsorbed on (100) facelets and terraces are downward shifted of about 28−30 cm^{-1} with respect to the gas phase, whereas those due to H_2 adsorbed on defects (edges?) are downward shifted of about 51−55 cm^{-1}; (iii) hydrogen adsorbed on (100) facets and terraces still keeps rotational mobility at 10 K; (iv) hydrogen adsorbed on defects is behaving as a severely hindered rotator; (v) on (100) faces the H−H axis of the adsorbed

molecule is parallel to the surface; (vi) the adsorption enthalpy results to be about 3 kJ/mol for smooth surfaces and 5.4 kJ/mol for defective films; (vii) in the adsorbed state the *ortho*/*para* ratio can vary with respect to the gas phase, depending on the temperature and the surface coverage.

Molecular $M^{n+}\cdots H_2$ (M^{n+} = alkali or alkali earth ion) adducts, similar to those found on the NaCl surface, are formed in zeolites and zeolitic materials at 77 K. The vibrational spectroscopy of such complexes has been widely studied mainly by Kazansky and co-workers;[6,29−32] complementary investigations in a wider temperature interval have been also performed by Cohen de Lara et al.[33,34] From these studies, the heat of adsorption of H_2 on the Na^+-exchanged zeolites has been found to be of the order of 10 kJ/mol. A very intense spectrum due to Na^+/H_2 adducts has been also obtained on the Na-ETS10 zeotype.[7] In all of the cases, it has been concluded that the forces involved in the $M^{n+}\cdots H_2$ interaction are mainly electrostatic and that under their action the ν(HH) stretching mode is becoming IR active. The perturbation of the ν(HH) mode observed in intrazeolitic adducts is larger than that observed for the $Na^+\cdots H_2$ complexes formed on (100) terraces of NaCl and is similar to that of H_2 complexes formed at surface defects (edges, steps, and corners), where the coordination number of the involved cations is lower and polarizing field consequently larger. We can see here that the influence of ligation on the ν(HH) mode of dihydrogen is analogous in surface complexes and in complexes formed in matrixes.

Vibrational Properties, Nature and Location of Dissociatively, and Molecularly Adsorbed Hydrogen Species on MgO. As seen in the Results section, dissociative adsorption of H_2 on MgO results in the formation of three families of hydroxyls and hydrides groups absorbing at 3712 and 1125, 3576−3547 and 1430−1418, and 3454 and 1325 cm^{-1}, where the first figure of each couple is the frequency of the ν(OH) mode and the second of the ν(MgH).

Considering the OH species first, two of them (absorbing at 3712 and 3454 cm^{-1}) are formed already at 20 K, whereas a third family (responsible for the doublet at 3576−3547 cm^{-1}) is formed only upon cooling the H_2/MgO system below 200−180 K after dosage of hydrogen at room temperature. Following the considerations developed in the previous paragraph, we can reasonably assume that the bands at 3712, 3576−3547 (doublet) and at 3454 cm^{-1} correspond to the IR modes of hydrogen fragments bonded to one, two, and three oxygen ions, respectively. It is worth underlining that in multiply bonded structures the H^+ fragment is not necessarily equally shared by the two (three) anionic sites. Most probably, the fragment is preferentially localized or more tightly bonded to one of the O^{2-} and interacting by hydrogen bonding with the other (others). This view is in agreement with the relative fwhm (full width at half maximum) of these bands which greatly increases (of at least three times) on passing from the 3712 to the 3454 cm^{-1} component: an increase of the fwhm, together with a bathochromic shift of the ν(OH) mode (as observed here), is in fact the typical spectroscopic manifestation expected on passing from linear O−H groups to hydrogen bonded −O−H···O− species. Structural situations such as those cited above can be found at corners, inverse (monatomic or larger) steps, and inverse corners where one, two, and three low coordinated O^{2-} are present. These basic sites act as preferential centers for the localization of the H^+ fragment. In a similar way, when the hydride species are considered, we can assume that the bands at 1430−1418, 1325, and 1125 cm^{-1} correspond to the vibrations of H^- fragments bonded to one, two, and three Mg^{2+} cations. As in the O^{2-} case, these situations can be found at corners, inverse (monatomic or larger) steps, and inverse corners where one, two, and three low-coordinated Mg^{2+} ions are present. These sites act as traps for the H^- fragment. The examination of the morphology of *hsa* MgO (ex-$Mg(OH)_2$), as resulting from Figures 1−3, is of great help in evaluating the soundness of the previous assignments. In fact, all of the structural situations cited above are simultaneously present on surfaces characterized by interpenetrated small cubes (as shown schematically in Figure 3b). As the H^+ and H^- fragments can be mobile on the surface, we cannot exclude that the sites of their final location could be different from those where dissociation occurred.

SCHEME 3

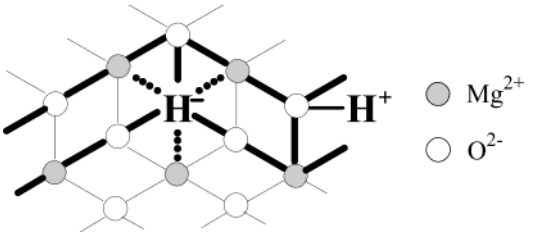

To try to establish a more detailed correlation between the observed band pairs and the structure of the sites involved in the H_2 splitting reaction, we can start considering first the most stable hydroxyl and hydride species, i.e., those irreversibly formed upon adsorption of H_2 at room temperature as well as at 20 K and responsible for the narrow absorption at 3712 cm^{-1}, due to the ν(OH) stretching mode, and the broad band at 1125 cm^{-1}, due to the ν(MgH) mode. Following the consideration developed so far, they are associated with H^+ fragments bonded to single O_{3c}^{2-} ions and to a H^- species bonded to three Mg^{2+} cations. This situation can occur on structural pairs formed by an anionic inverse corner site plus an oxygen corner site as shown in Scheme 3.[21]

Whether the $\square_{3c}^-$ pseudo-vacancy and the O_{3c}^{2-} site are adjacent (like in Scheme 3) or distant is difficult to be inferred from the spectroscopic data. It is however a matter of facts that the composite structure of the absorption centered at 3712 cm^{-1} and the broad character of the hydride band at 1125 cm^{-1} seem to suggest that we are dealing with a multiplicity of structurally similar species possibly characterized by variable $\square_{3c}^-\cdots O_{3c}^{2-}$ distances. It is worth underlining that the adsorption process generating the 3712−1125 cm^{-1} doublets is characterized by negligible activation energy, because the involved H^+ and H^- species are immediately formed at temperature as low as 20 K.

On the basis of the assignment of the 3712−1125 cm^{-1} pair, we can now proceed to tentatively single out the sites where the hydroxyl-hydride pairs absorbing at 3454−1325 cm^{-1} are located. From previous considerations we know that the 3454 cm^{-1} band is due to a H^+ fragment adsorbed at a tricoordinated $\square_{3c}^+$ pseudo-vacancy located at an inverse corners, while the 1325 cm^{-1} band is due to a H^- species coordinated to two Mg^{2+} ions. On this basis the structure of the sites and of the species responsible for the 3454−1325 cm^{-1} pair is well represented in Scheme 4a (where, as already outlined before, the H^+ fragment is not necessarily equally shared by the three anions). These structures are the second in term of stability. This hypothesis is fully confirmed by the observation of the molecularly adsorbed precursor, absorbing at frequency as low as 4031 cm^{-1} (Figure 9) and hence characterized by a substantial polarization and elongation of the H−H bond as expected for a molecular structure like that represented in Scheme 4b.

Coming now to the bands in the 3576−3547 and 1430−1418 cm^{-1} intervals, the hypothetical structure of the adsorbing site

SCHEME 4

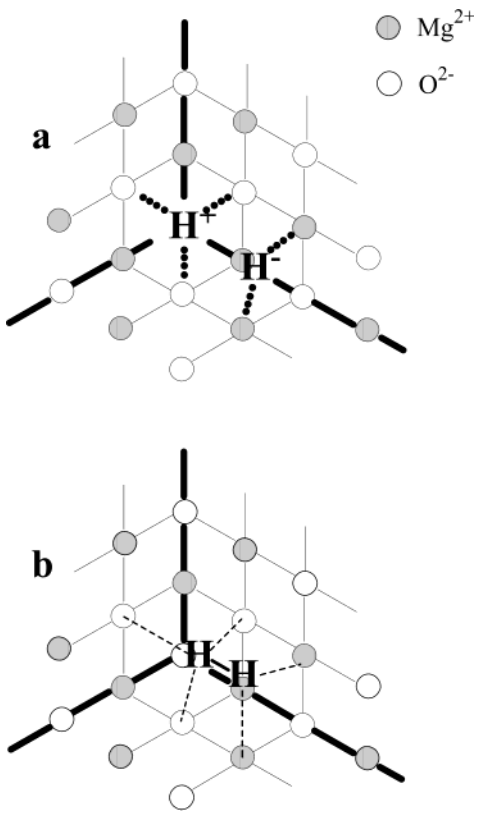

SCHEME 5

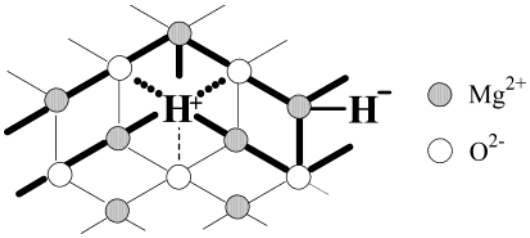

is represented in Scheme 5. This structure is analogous to that in Scheme 3, the only difference being that at the inverse corner a positive $\square_{3c}^{+}$ pseudo-vacancy is now located.

In this structure, the H^- fragment is adsorbed on a Mg_{3c}^{2+} ion located on a corner, thus justifying the 1430−1418 cm^{-1} absorption. The H^+ fragment is actually tri-coordinated, but being strongly bonded to two O_{4c}^{2-} ions and more loosely to one O_{5c}^{2-}, it behaves as bi-coordinated H^+ species (so justifying the 3576−3547 cm^{-1} absorption). The composite structure of the 3576−3547 and 1430−1418 cm^{-1} bands could derive from the possibility of the $\square_{3c}^{+}$ vacancy and the Mg_{3c}^{2+} ion to be either adjacent or placed at variable distances.

From the previous discussion, it follows that only the O^{2-} and Mg^{2+} ions located at inverse corner sites are able to dissociate H_2. This implies that not all the 3-fold surface ions are involved in hydrogen splitting: this is for instance the case of those ions located on edges and corners of regular (or little interpenetrated) small cubes. As it will be shown now, these sites are involved in the adsorption of hydrogen in molecular form.

Before discussing this point, it is useful to recall that natural hydrogen is constituted by 1/4 of *para*-H_2 (i.e., molecules for which $I = 0$, where I is the nuclear momentum, and the rotational quantum number can only assume the values $J = 0$, 2, 4, ...) and by 3/4 of *ortho*-H_2 ($I = 1$ and $J = 1$, 3, 5, ...). In the gas phase the ν(HH) frequencies of the two forms fall at different values (4161.1 cm^{-1} for *para*- and 4155.2 cm^{-1} for *ortho*-H_2), corresponding to a difference $\Delta\bar{\nu} = 5.9$ cm^{-1}.[49] A similar difference (6 cm^{-1}) has been observed for dihydrogen trapped in Ar matrix.[50,51]

Going to the H_2/MgO system, the spectrum of hydrogen molecularly adsorbed on *hsa* MgO (Figure 7) can be roughly divided into three regions: 4150−4000 cm^{-1} (I); 4350−4150 cm^{-1} (II) and 4800−4350 cm^{-1} (III). On the basis of the literature (see for example[6,24−26]), we can reasonably assume that: i) the ν(HH) bands of *orto*- and *para*- hydrogen adsorbed on (100) facelets and terraces and on other defects are expected to fall in the first interval (4150−4000 cm^{-1}) (*vide infra*); ii) the combinations of the ν(HH) stretching with the frustrated translational modes of adsorbed H_2 in the second region (4350−4150 cm^{-1}) and that iii) the rotovibrational components of adsorbed *para*- and *ortho*-hydrogen (respectively falling in the free molecule at $\bar{\nu} = \bar{\nu}$ (HH) + 10B and $\bar{\nu} = \bar{\nu}$ (HH) + 6B cm^{-1}, where B = 60 cm^{-1} is the H_2 rotational constant) have to be expected in the 4800−4700 cm^{-1} (*para*) and in the 4500−4400 cm^{-1} (*ortho*-hydrogen) intervals.

To distinguish the manifestations due to hydrogen molecularly adsorbed on (100) faces and terraces from those due to H_2 adducts formed on more defective situations, it is useful to compare the spectra obtained at maximum coverage on *hsa* and *smoke* MgO (Figure 8). From this comparison it can be inferred that the band centered at 4123 cm^{-1} (complex, possibly because of *ortho*/*para* splitting) is certainly due to H_2 adsorbed on the (100) faces and terraces as it is clearly observed on *smoke* as well as on *hsa* MgO. It is also worth noticing that this absorption is formed only at the highest pressures (Figures 4 and 8), as expected for species involving low energetic sites such as those exposed on low index crystallographic planes. The given assignment is also in agreement with the literature data concerning H_2 adsorbed on the (100) NaCl system.[24,25,27] Let us mention the presence in the spectra of Figure 7 of a band at 4215 cm^{-1}, which shows an intensity vs pressure behavior similar (at least at low-medium coverage) to that of the absorption at 4123 cm^{-1}. Based on the literature,[24,25,27] we tentatively assign it to the combination of the ν(HH) motion of adsorbed hydrogen with the frustrated translation of the molecule along the direction perpendicular to the surface (which should be therefore located at about 90 cm^{-1}). On approaching the maximum H_2 equilibrium pressure at 20 K, i.e., in conditions where multilayer adsorption is expected to occur, the 4215 cm^{-1} band broadens and then merges into a wide absorption covering the 4400−4200 cm^{-1} interval: in our opinion, this behavior is due the perturbation of the frustrated translational motions of the adsorbed H_2 molecules when becoming surrounded by liquid like species. It is finally noticeable the appearance at medium-high coverge (in connection with the above-discussed manifestations) of rotovibrational components located in the 4800−4700 cm^{-1} range. Their impressive intensity indicates that even at 20 K the hydrogen molecules adsorbed on (100) faces and terraces still possess rotational freedom. As far as the structure of H_2 adsorbed on (100) faces and terraces is concerned, we are in favor of an interaction with the 5-fold coordinated Mg^{2+} cations following a side-on configuration. This hypothesis is in agreement with the structure proposed for H_2 adsorption on (100) NaCl;[24,25,27] the side-on geometry is also supposed to be the most stable for $M^+(H_2)$ complexes formed in cryogenic matrixes.[52,53]

Moving now to the doublet at 4106−4100 cm^{-1}, it shows a more pronounced decrease in intensity upon reducing the MgO

surface area (Figure 8) as compared with the band at 4123 cm^{-1}. Together with the lower intensity, this allows its assignment to H_2 molecules adsorbed on 4-fold coordinated Mg^{2+} ions (located on edges and steps), the presence of two components separated by 6 cm^{-1} being due to *ortho/para* splitting. The shift of the ν(HH) mode in the $Mg_{4c}^{2+}\cdots H_2$ adducts with respect to the free H_2 molecule ($\Delta\bar{\nu} = -58$ cm^{-1}) well compares with the data concerning H_2 adsorption on similar defects at the NaCl surface.[24,25,27] As it is clearly observable in the inset of Figure 7, the relative intensity of the components of the doublet is dramatically changing with the H_2 equilibrium pressure: this means that the *orto*/*para* ratio in the adsorbed state is coverage dependent. This subtle phenomenon, which will be no further discussed in this paper, has been already observed for the H_2/NaCl system.[24−27] We hypothesize that also in this case hydrogen is adsorbed on the Mg_{4c}^{2+} ions in side-on configuration. Two broad and intense absorptions at 4167 (becoming a doublet at the highest pressures, just before disappearing) and 4257 cm^{-1} clearly behave, at low H_2 coverage, as the 4106−4100 cm^{-1} doublet (Figure 7). We think that the most plausible interpretation of these manifestation is in terms of combination between the ν(HH) vibration of the $Mg_{4c}^{2+}\cdots H_2$ adducts and the frustrated translations of the adsorbed molecule along ($\bar{\nu} \sim 60$ cm^{-1}) and perpendicularly to the edge direction ($\bar{\nu} \sim 150$ cm^{-1}). Similar explanation has been given for an intense band at 4164 cm^{-1} observed by H_2 adsorption on defective NaCl films[24,25] where the in plane frustrated translation is occurring at ca. 55 cm^{-1}. In this hypothesis, however, an interesting question arises concerning the intensity of the combination mode at 4167 cm^{-1}: in fact, it appears larger than the intensity of the fundamental H−H stretching at 4106−4100 cm^{-1} (but the same also holds for the band at 4257 cm^{-1}). A plausible explanation for this apparent anomaly is as follows: while the ν(HH) fundamental is intrinsically very weak in the adsorbed state because deriving from an IR inactive mode of the unperturbed molecule, the surface-H_2 modes (frustrated translations) are intrinsically active. Consequently, the ν(HH) + ν(surface-H_2) combination modes gain intensity and can become more pronounced than the ν(HH) fundamental. The progressive broadening and final merging of these bands into wider structureless absorptions (clearly observable at the highest pressures) is again the consequence of the formation of a multilayer of adsorbed hydrogen and subsequent solvation of the H_2 molecule bonded to the Mg^{2+} centers (whose translational motions are heavily perturbed).

Among the remaining features of Figure 7, it is most noticeable the strong and narrow doublet at 4081−4075 cm^{-1}, already present at very low pressure and merging into a broader feature centered at 4070 cm^{-1} when the coverage is increased. As the separation of the components of the doublet is the same as that expected for *ortho/para* splitting (6 cm^{-1}), it is assigned to *ortho*- and *para*-hydrogen molecules adsorbed on the same kind of sites. This assignment is also in agreement with the observation that the ν(HH) modes of the two species are identically downward shifted by about 80−81 cm^{-1} with respect to gaseous H_2. The shift is actually larger than that observed for hydrogen adsorbed on the (100) planes ($\Delta\bar{\nu} = -38$ cm^{-1}) and on edges and steps ($\Delta\bar{\nu} = -58$ cm^{-1}) and hence more defective situations must be invoked like 3-fold coordinated Mg_{3c}^{2+} sites on corners. Assignment of the 4081−4075 cm^{-1} doublet to $Mg_{3c}^{2+}\cdots H_2$ adducts on corners is supported by the observation that these bands readily disappear upon sintering (Figure 8). It is noteworthy that shifts as large as 80 cm^{-1} have not been observed on NaCl films:[24] the reason lies in the fact that hydrogen adsorbed on the highly coordinatively unsaturated divalent Mg^{2+} ions on corners experiences a polarizing field than definitely larger than that of H_2 adsorbed on monovalent Na^+; this in turn indicates that only electrostatic forces are involved in the adsorption process.[54] The disappearance of the 4081−4075 cm^{-1} doublet at high H_2 pressure can be ascribed to the addition of a further H_2 molecules to the 3-fold coordinated $Mg_{3c}^{2+}\cdots H_2$ species. As in this conditions multilayer adsorbed hydrogen is also present, the effect of adsorbate−adsorbate interactions must be also taken into account. In conclusion, the progressive disappearance of the original doublet and the formation of the broad feature centered at 4070 cm^{-1} is due to both the above effects acting together. In this respect it is worth recalling that multiple addition of molecular species to unsaturated Mg_{3c}^{2+} ions is a well-known phenomenon for the MgO/CO system.[37,55] Two minor narrow features at 4145 and 4200 cm^{-1} seem to behave like the 4081−4075 cm^{-1} doublet upon pressure changes; without entering into excessive details, we think that a plausible interpretation for these absorption can be in terms of combination modes involving frustrated translations (in analogy with the previous assignments, vide supra).

Based on the arguments developed so far about the molecular species, it is interesting to re-consider now the transient feature at 4031 cm^{-1} which, as we have seen, can be assigned to H_2 molecularly adsorbed at inverse corners. The facts that (i) this band is shifted to a frequency definitely lower of that of molecular hydrogen adsorbed on defects such as edges and corners and on (100) planes (all falling in the 4150−4070 cm^{-1} spectral region) and (ii) the dissociation process proceeds on these sites at a temperature as low as 20 K demonstrate that we are dealing with surface centers where dihydrogen is strongly polarized, which indeed is what one can expect for structures such as that shown in Scheme 4b. On this basis, the weak band observed at 4060 cm^{-1} in Figure 7 could be analogously ascribed to a second family of inverse sites, whose interaction energy is slightly higher. We advance the (highly) tentative hypothesis that these molecular species could be the precursors of the hydride and hydroxyl groups (formed upon heterolytic dissociation) absorbing at 1430−1418 and 3576−3547 cm^{-1}.

As a final observation, let us comment that, when the overall intensity of the spectrum of hydrogen adsorbed directly at 20 K is compared (at maximum coverage) with that of the spectrum obtained by H_2 dosage at room temperature and subsequent cooling at 20 K, the differences appear negligible. This means that the presence in the second case of the "additional" dissociated species responsible for the bands at 3454 and 1325 cm^{-1} do not substantially alter the population of the molecular adducts. In other words the concentration of these dissociatively adsorbed species is so low that their presence or absence has no effect on the population of the molecular species adsorbed on the more common surface terminations.

Thermodynamic Properties of the $Mg^{2+}\cdots H_2$ Molecular Adducts. The IR cell used in this investigation allows us to obtain the IR spectrum of H_2 adsorbed at the temperature variable in the 300−20 K interval and fixed (or, in general, controlled) equilibrium pressure. From the sequence of spectra recorded in the experiments where H_2 is dosed on MgO at 300 K and the temperature is then lowered in steps down to 20 K, it is possible to measure the intensity A (as a function of the temperature) of the bands due to molecular adsorption of hydrogen on specific surface sites following the equilibrium $Mg_{nc}^{2+} + H_2 \rightleftarrows Mg_{nc}^{2+}\cdots H_2$ (where $n = 3$ for corner sites, 4

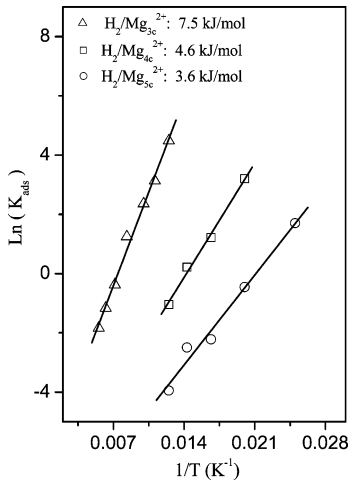

Figure 10. Dependence of $\ln(K_{ads})$ on $(1/T)$ for H_2 molecularly adsorbed on the Mg_{3c}^{2+} (△), Mg_{4c}^{2+} (□) and on Mg_{5c}^{2+} (○) defective sites at the surface of *hsa* MgO.

for edge and step sites and 5 for sites on (100) faces and terraces). Once $A(T)$ (intensity vs temperature) is obtained, the function θ(T) (surface coverage vs temperature) can be derived from the ratio $\theta(T)=A(T)/A_{max}$, where A_{max} is the maximum intensity of the absorption band for a given $Mg_{nc}^{2+}\cdots H_2$ species. As[56,57]

$$K_{ads} = \frac{\theta(T)}{[1-\theta(T)]\cdot p_{H_2}}$$

where K_{ads} is the equilibrium constant and p_{H_2} the equilibrium pressure, it follows that the H_2 adsorption energy can be measured from the spectroscopic data by a linear plot of $ln(K_{ads})$ vs $(1/T)$ (see ref 37 for further details). The plots of the data concerning the *hsa* MgO/H_2 system are reported in Figure 10.

For the $Mg_{4c}^{2+}\cdots H_2$ adducts, the intensity of the ν(HH) + ν(surface-H_2) combination (band at 4167 cm^{-1}) has been actually used in place of the ν(HH) fundamental mode at 4106−4100 cm^{-1}, because of the difficulties in the determination in the latter case of the maximum intensity (A_{max}). Furthermore, as the bands due to hydrogen adsorbed on the various sites are always constituted by more or less resolved doublets (due to the *ortho/para* splitting), the integrated intensity obtained by summing the contribution of both components has been used (with the implicit reasonable assumption that the complexes of the two hydrogen isomers have the same extinction coefficient). From the linear plots shown in Figure 10, the H_2 adsorption enthalpies are 3.6 kJ/mol on the pentacoordinated Mg^{2+} ions emerging on the (100) faces and terraces, 4.6 kJ/mol on tetracoordinated cations placed on edges and steps, and 7.5 kJ/mol on tri-coordinated cations located on the corners. The 3.6 kJ/mol value found for the $Mg_{5c}^{2+}\cdots H_2$ adducts is in good agreement with the experimental (3.4 ± 0.8 kJ/mol)[24,26] and theoretical (2.7−3.4 kJ/mol for the *para-ortho* species)[26] values concerning H_2 adsorption on the surface of NaCl (leading to the obvious conclusion that, as on NaCl, the interaction of H_2 with the MgO surface is purely electrostatic). The higher adsorption enthalpy on edges and steps (4.6 kJ/mol) and on corners (7.5 kJ/mol) is a consequence of the increased electrostatic field exerted by these sites. The value found for adsorption on tri-coordinated Mg_{3c}^{2+} ions located on corners is comparable with that obtained for H_2 adsorbed on the highly polarizing Na^+ cations of Na-A zeolite (about 10 kJ/mol).[58]

Conclusions

The FTIR investigation of the H_2 adsorption, in the 300−20 K temperature interval, on MgO samples with specific surface area comprised between ∼230 to ∼10 m^2/g, allows us to conclude the following:

(a) In the 80−20 K interval, H_2 is reversibly adsorbed in molecular form on the Mg_{5c}^{2+} (pentacoordinated sites on extended (100) faces), Mg_{4c}^{2+} (tetracoordinated sites on steps and corners), and Mg_{3c}^{2+} (tri-coordinated sites on edges) ions emerging at the surface of the small cubes or cubic microstructures typical of polycrystalline MgO with the formation of $Mg_{nc}^{2+}\cdots H_2$ adducts.

(b) The formation enthalpy of the above molecular complexes, as measured by spectroscopic runs performed at variable temperature and constant H_2 pressure, is in the range 3.6−7.5 kJ/mol.

(c) Transient molecular adducts evolving at 20 K toward irreversible hydroxyl and hydride species, are also formed on $[(Mg_{5c}^{2+})_2(O_{5c}^{2-})_3]$ clusters present on inverse corners.

(d) Three different families of $O^{2-}H^+$ and $Mg^{2+}H^-$ surface species are formed by heterolytic splitting of H_2 (one of them being never observed in previous studies) on inverse corners and edges.

References and Notes

(1) Zecchina, A.; Scarano, D.; Bordiga, S.; Spoto, G.; Lamberti, C. *Adv. Catal*. **2001**, *46*, 265.
(2) Schlapbach, L.; Züttel, A. *Nature* **2001**, *414*, 353.
(3) Stone, F. S.; Garrone, E.; Zecchina, A. *Mater. Chem. Phys.* **1985**, *13*, 331.
(4) Nijkamp, M. G.; Raaymakers, J. E. M. J.; van Dillen, A. J.; de Jong, K. P. *Appl. Phys. A* **2001**, *72*, 619.
(5) Rosi, N. L.; Eckert, J.; Eddaoudi, M.; Vodak, D. T.; Kim, J.; O'Keeffe, M.; Yaghi, O. M. *Science* **2003**, *300*, 1127.
(6) Kazansky, V. B. *J. Mol. Catal. A-Chem.* **1999**, *141*, 83.
(7) Zecchina, A.; Otero Arean, C.; Palomino, G. T.; Geobaldo, F.; Lamberti, C.; Spoto, G.; Bordiga, S. *Phys. Chem. Chem. Phys.* **1999**, *1*, 1649.
(8) Coluccia, S.; Boccuzzi, F.; Ghiotti, G.; Morterra, C. *J. Chem. Soc., Faraday Trans. 1* **1982**, *78*, 2111.
(9) Knözinger, E.; Jacob, K. H.; Hofmann, P. *J. Chem. Soc., Faraday Trans.* **1993**, *89*, 1101.
(10) Kazansky, V. B.; Borovkov, V. Y.; Kustov, L. M. *Proceedings of the 8th Internations Congress on Catalysis*; Berlin, West Germany, 1984.
(11) Kazansky, V. B.; Borovkov, V. Y.; Zaitsev, A. V. *Proceedings of the 9th International Congress on Catalysis*; Calgary, Canada, 1988.
(12) Coluccia, S.; Boccuzzi, F.; Ghiotti, G.; Mirra, C. *Z. Phys. Chem. Neue Folge.* **1980**, *121*, 141.
(13) Diwald, O.; Hofmann, P.; Knözinger, E. *Phys. Chem. Chem. Phys.* **1999**, *1*, 713.
(14) Cavalleri, M.; Pelmenschikov, A.; Morosi, G.; Gamba, A.; Coluccia, S.; Martra, G. *Stud. Surf. Sci. Catal.* **2001**, *140*, 131.
(15) Diwald, O.; Berger, T.; Sterrer, M.; Knozinger, E. *Stud. Surf. Sci. Catal.* **2001**, *140*, 237.
(16) Sterrer, M.; Berger, T.; Diwald, O.; Knozinger, E. *J. Am. Chem. Soc.* **2003**, *125*, 195.
(17) Diwald, O.; Knözinger, E. *J. Phys. Chem. B* **2002**, *106*, 3495.
(18) Chiesa, M.; Paganini, M. C.; Giamello, E.; Di Valentin, C.; Pacchioni, G. *Angew. Chem.-Int. Ed.* **2003**, *42*, 1759.
(19) Garrone, E.; Stone, F. S. *J. Chem. Soc., Faraday Trans. 1* **1987**, *83*, 1237.
(20) Paganini, M. C.; Chiesa, M.; Giamello, E.; Coluccia, S.; Martra, G.; Murphy, D. M.; Pacchioni, G. *Surf. Sci.* **1999**, *421*, 246.
(21) Ricci, D.; Di Valentin, C.; Pacchioni, G.; Sushko, P. V.; Shluger, A. L.; Giamello, E. *J. Am. Chem. Soc.* **2003**, *125*, 738.
(22) Niu, J.; Rao, B. K.; Jena, P.; Manninen, M. *Phys. Rev. B* **1995**, *51*, 4475.
(23) Sweany, R. L.; Vuong, L.; Bishara, J. *J. Phys. Chem. A* **2002**, *106*, 11440.
(24) Dai, D. J.; Ewing, G. E. *J. Chem. Phys.* **1993**, *98*, 5050.
(25) Heidberg, J.; Gushanskaya, N.; Schönekäs, O.; Schwarte, R. *Surf. Sci.* **1995**, *331−333*, 1473.
(26) Briquez, S.; Picaud, S.; Girardet, C.; Hoang, P. N. M.; Heidberg, J.; Vossberg, A. *J. Chem. Phys.* **1998**, *109*, 6435.

(27) Heidberg, J.; Vossberg, A.; Hustedt, M.; Thomas, M.; Briquez, S.; Picaud, S.; Girardet, C. *J. Chem. Phys.* **1999**, *110*, 2566.
(28) Dai, D. J.; Ewing, G. E. *J. Chem. Phys.* **1994**, *100*, 8432.
(29) Kazansky, V. B.; Borovkov, V. Y.; Serich, A.; Karge, H. G. *Micropor. Mesopor. Mater.* **1998**, *22*, 251.
(30) Kazansky, V. B.; Jentoft, F. C.; Karge, H. G. *J. Chem. Soc., Faraday Trans.* **1998**, *94*, 1347.
(31) Bordiga, S.; Garrone, E.; Lambert, C.; Zecchina, A.; Arean, C. O.; Kazansky, V. B.; Kustov, L. M. *J. Chem. Soc., Faraday Trans.* **1994**, *90*, 3367.
(32) Kustov, L. M.; Borovkov, V. Y.; Kazansky, V. B. *Kinetika i Kataliz* **1984**, *25*, 471.
(33) Stephanie-Victoire, F.; Goulay, A. M.; Cohen de Lara, E. *Langmuir* **1998**, *14*, 7255.
(34) Stephanie-Victoire, F.; Cohen de Lara, E. *J. Chem. Phys.* **1998**, *109*, 6469.
(35) Otero Arean, C.; Manoilova, O. V.; Bonelli, B.; Rodríguez Delgado, M.; Turnes Palomino, G.; Garrone, E. *Chem. Phys. Lett.* **2003**, 370.
(36) Sigl, M.; Ernst, S.; Weitkamp, J.; Knözinger, H. *Catal. Lett.* **1997**, *45*, 27.
(37) Spoto, G.; Gribov, E.; Ricchiardi, G.; Damin, A.; Scarano, D.; Bordiga, S.; Lamberti, C.; Zecchina, A. *Prog. Surf. Sci.* **2004**, in press.
(38) Coluccia, S.; Lavagnino, S.; Marchese, L. *Mater. Chem. Phys.* **1988**, *18*, 455.
(39) Knözinger, E.; Jacob, K.-H.; Singh, S.; Hofmann, P. *Surf. Sci.* **1993**, *290*, 388.
(40) Aldridge, S.; Downs, A. J. *Chem. Rev.* **2001**, *101*, 3305.
(41) Hinde, R. J. *J. Phys. Chem. A* **2000**, *104*, 7580.
(42) Tague, T. J.; Andrews, L. *J. Phys. Chem.* **1994**, *98*, 8611.
(43) MacKay, K. In *Comprehensive Inorganic Chemistry*; Bailer, J. C., Emeleves, H. J., Nikolm, R., Trotman-Oichenson, A. J., Eds.; Pergamon Press: Oxford, 1973; Vol. 1, p 23.
(44) Shido, T.; Asakura, K.; Iwasawa, Y. *J. Chem. Soc., Faraday Trans. I* **1989**, *85*, 441.
(45) Beckenkamp, K.; Lutz, H. D. *J. Mol. Struct.* **1992**, *270*, 393.
(46) Hermansson, K. *J. Chem. Phys.* **1991**, *95*, 3578.
(47) Simandiras, E. D.; Nicolaides, C. A. *Chem. Phys. Lett.* **1991**, *185*, 529.
(48) Nicolaides, C. A.; Simandiras, E. D. *Chem. Phys. Lett.* **1992**, *196*, 213.
(49) Schwartz, C.; LeRoy, R. J. *J. Mol. Spectrosc.* **1987**, *121*, 420.
(50) Warren, J. A.; Smith, G. A.; Guillory, W. A. *J. Chem. Phys.* **1980**, *72*, 4901.
(51) Chan, M.; Lee, S.; Okomura, M.; Oka, T. *J. Chem. Phys.* **1981**, *95*, 88.
(52) McKee, M. L.; Sweany, R. L. *J. Phys. Chem. A* **2000**, *104*, 962.
(53) Dixon, D. A.; Gole, J. L.; Komornicki, A. *J. Phys. Chem.* **1988**, *92*, 1378.
(54) Folman, M.; Kozirovski, Y. *J. Colloid Interface Sci.* **1972**, *38*, 51.
(55) Pelmenshikov, A. G.; Morosi, G.; Gamba, A.; Coluccia, S. *J. Phys. Chem.* **1995**, *99*, 15018.
(56) Paukshtis, E. A.; Yurchenko, N. E. *Russ. Chem. Rev.* **1983**, *52*, 426.
(57) Otero Areán, C.; Manoilova, O. V.; Bonelli, B.; Delgado, M. R.; Palomino, G. T.; Garrone, E. *Chem. Phys. Lett.* **2003**, *370*, 631.
(58) Koubi, L.; Blain, M.; Cohen de Lara, E. *Chem. Phys. Lett.* **1994**, *217*, 544.